Bacterial species and surface structures shape gene transfer and the transcriptional landscape during active conjugation

Galain C Williams[1], Jillian C Danne[2], Simon Crawford[2], Jihane Homman-Ludiye[3], Xenia Kostoulias[4], Bailey Heron[1], Tasnia Islam[1], Melvin Yong[5], Yunn-Hwen Gan[5], Yogitha N Srikhanta[1,6] and Dena Lyras[1,6†]

[1]Infection Program, Monash Biomedicine Discovery Institute and Department of Microbiology, Monash University, Clayton, Victoria Australia, 3800.

[2]Monash Ramaciotti Centre for Cryo-Electron Microscopy, A Node of Microscopy Australia, Monash University, Clayton, Victoria, Australia, 3800.

[3]Monash Micro Imaging, Monash University, Clayton, Victoria, Australia, 3800.

[4]Department of Infectious Diseases, The Alfred Hospital and School of Translational Medicine, Monash University, VIC, Australia, 3004

[5]Infectious Diseases Translational Research Program, Department of Biochemistry, Yong Loo Lin School of Medicine, National University of Singapore, Singapore, Singapore, 117596.

[6]Joint senior author; these authors contributed equally to this article

Corresponding Author: Professor Dena Lyras

Email: Dena.Lyras@monash.edu

Author Contributions: G.W. co-designed experiments, performed the majority of the experimental work and co-wrote the manuscript. J.D. and S.C. performed the TEM and assisted with SEM imaging. J.H. assisted with fluorescent microscopy imaging and analysis. X.K. assisted with RNA sequencing. B. H. assisted with fluorescent microscopy. T. I. assisted with conjugation time course experiments. M.Y. and Y.H.G assisted with the *K. pneumoniae* conjugation experiments and experimental design. Y.N.S. co-wrote manuscript & co-designed the majority of experiments. D.L. co-designed all experiments and co-wrote the manuscript.

Competing Interest Statement: No Competing Interests

Keywords: Bacterial Conjugation; Plasmid Transfer; Antibiotic Resistance; Broad host range plasmids; mobile genetic elements

Abstract

Conjugative plasmids drive bacterial evolution and niche adaptation, yet how their active acquisition reshapes host transcription remains poorly understood. Most studies focus on stable plasmid carriage, overlooking the dynamic transcriptional changes during conjugation itself. Here, we show that active RP4 conjugation triggers an immediate, host- and surface factor-dependent transcriptional response. This includes activation of non-SOS stress pathways, motility, exopolysaccharide production, anaerobic respiration, and metabolic adaptation. These responses do not inhibit conjugation, suggesting they serve to maintain host homeostasis. Capsule expression blocks these responses by preventing conjugation, and also inhibits RP4 activation by physically blocking donor-recipient contact. Unexpectedly, RP4 overcomes this barrier by exploiting single-cell variation in recipient capsule thickness, successfully conjugating with thin-capsulated recipients. These findings reveal a striking interplay between plasmid, host, and surface architecture in shaping the conjugation transcriptional landscape, with broad implications for plasmid dissemination and bacterial evolution.

53 **Main Text**

54 **Introduction**

55 Conjugative plasmids are key drivers of horizontal gene transfer, enabling rapid trait
56 acquisition in bacteria (1). Critically, their spread through bacterial populations is closely
57 linked to the rise of antibiotic resistance across clinical and environmental settings (2, 3).
58 Conjugation, the primary mechanism of plasmid dissemination, involves the transfer of
59 single-stranded plasmid DNA from a donor into a neighbouring recipient *via* a type IV
60 secretion system (4). Although traditionally viewed as a donor-driven process, recent
61 seminal studies have revealed that recipients play active, multifaceted roles in modulating
62 conjugation (5-8). For example, the capsule of *Klebsiella pneumoniae* inhibits transfer of
63 many plasmid types (8, 9), whilst *K. pneumoniae* outer membrane proteins act as
64 receptors that selectively engage cognate plasmid-bearing donors (7). Additionally,
65 plasmid carriage induces widespread changes in recipient chromosomal gene expression
66 (10), altering cellular functions beyond the plasmid's genetic content. These findings
67 highlight a complex interplay between donor, recipient and plasmid that shapes plasmid
68 dissemination and influences host cell physiology and evolution. In this study, we aimed
69 to further dissect this interplay during active conjugation of the broad host range plasmid
70 RP4.

71 Stable plasmid carriage is known to broadly reprogram host chromosomal gene
72 expression, affecting metabolic, respiratory, transport, virulence, and other pathways (10-
73 14). However, the transcriptional response of recipient cells during active conjugation,
74 particularly involving broad host range plasmids like RP4, remains poorly understood.
75 While many plasmids trigger an SOS response upon entry (15), RP4 does not strongly
76 activate this pathway (15), suggesting alternative mechanisms may be at play. Despite
77 RP4's widespread use in inter-species gene transfer, its transcriptional impact across
78 diverse species is surprisingly underexplored. For example, RP4 has been shown to
79 supress ammonia oxidation in environmental bacteria (16), but most studies have been
80 conducted in the presence of external compounds such artificial sweeteners (17), or
81 biochar (18), confounding the effects of RP4 acquisition with those of the compounds
82 themselves.

Research on other broad host range plasmids suggests that initial plasmid-host interactions can shape the outcome of transfer. In *Pseudomonas putida*, for instance, R388 transfer induces expression of the *hsdRMS* restriction system, which is counteracted by the R388 anti-restriction protein ArdC (19). Whether RP4 elicits a similar recipient-specific response, or encounters barriers to conjugation, remains unknown. Understanding how recipient species modulate RP4 conjugation is critical, as broad host range plasmids are major vectors in the spread of antibiotic resistance (20).

Beyond transcriptional responses, recipient bacteria also influence conjugation through their cell surface structures. Capsules, thick outer layers of polysaccharide, are well-established barriers to conjugation (8). Paradoxically, they are also associated with increased rates of horizontal gene transfer (21), suggesting a complex and unresolved relationship between capsule presence and gene exchange. This paradox remains poorly understood, in part because capsule-mediated inhibition of conjugation has only been demonstrated in *Klebsiella* species, and the underlying mechanisms are yet to be elucidated.

Using an innovative liquid displacement method to infer capsule volume (8), Haudiquet *et al* showed that larger capsule serotypes more strongly inhibit plasmid transfer, implicating capsule length as a key factor. Given that cell-to-cell contact is essential for RP4 conjugation (22), a plausible, though unproven, hypothesis is that capsules physically obstruct donor-recipient contact, thereby preventing conjugation. To deepen our understanding of how recipient bacteria respond to and modulate broad host range plasmid conjugation, we investigated the transcriptional and structural impact of active RP4 transfer in *Escherichia coli* and *K. pneumoniae*. Both species exhibited distinct transcriptional responses involving diverse host functions including anaerobic respiration, non-SOS stress adaptation, and substrate transport. Notably, the *K. pneumoniae* response was only observed in the absence of capsule, revealing a previously unrecognised role for the capsule in suppressing host transcriptional reprograming during conjugation.

RP4 gene expression was also influenced by the recipient species and was inhibited by the presence of capsule. We confirmed that capsule blocks conjugation across diverse

113 recipients by preventing donor-recipient cell-to-cell contact. Surprisingly, RP4 could
114 exploit single cell variation in capsular thickness to facilitate transfer, bypassing the need
115 for a capsular serotype switch. These findings provide a unified framework for
116 understanding how recipient species and their surface structures shape the transcriptional
117 landscape and dissemination of broad host range plasmids.

118 **Results**

119 **Active RP4 conjugation elicits triggers non-SOS stress, respiratory and metabolic**
120 **reprogramming**

121 To map the transcriptional landscape of RP4 conjugation, we first distinguished active
122 conjugation from transconjugant vertical inheritance using a time-course assay (Fig 1a).
123 At 15 minutes, new transconjugants were actively generated without changes in recipient
124 population size, confirming this as a window of active conjugation and ruling out vertical
125 inheritance as a confounding factor. We then performed RNA-seq on a conjugating
126 mixture of laboratory donor *E. coli* LT101(pVS520) and a genetically distant clinical
127 recipient, *E. coli* DLL7555. For comparison, RNA was also extracted from mock
128 conjugations lacking pVS520, and from donor monocultures. The >78,000 core genome
129 differences between DLL7555 and LT101 enabled accurate, strain-specific read
130 assignment using a concatenated LT101-DLL7555 reference genome.

131 RP4 conjugation triggered differential expression of 130 genes in the *E. coli* recipient (Fig
132 1b), including those involved in adaptation to external stressors such as temperature
133 shock (*cspG*, *hslJ, deaD*), pH regulation (*yagU, ygaC, ybay, speF*), osmotic stress (*osmB,*
134 *osmY, nhaA*), and other stress-related pathways (*mliC, soxS, rcsA, phoR*). This was
135 accompanied by upregulation of genes involved in colanic acid biosynthesis (*wzc, wzb,*
136 *cpsB, wcaJ, wcaI, wcaE, wcaC, wcaA, gmd, fcl, wza, wcaD*), exopolysaccharide
137 production (*yjbG, yjbF, yjbH*), and flagella assembly (*fliN, fliM, flgG, flgF, glgI, flgH, flhA,*
138 *fliO*).

139 Although conjugative plasmids are known to promote biofilm formation (23), we observed
140 decreased expression of the biofilm master regulator *csgD*. Consistently, co-culture of
141 DLL7555 with LT101(pVS520) resulted in a slight but significant reduction in biofilm

142 formation compared to both LT101 co-culture or monoculture conditions (Supplementary
143 Fig 1).

144 RP4 conjugation also induced upregulation of genes involved in anaerobic respiration and
145 energy generation (*fdnI, dmsB, napC, narG, narH, narI, hycF, nrfA, nrfD, nrfC, nirB, fumB,*
146 *dcuC*), overlapping with pathways linked to inorganic nutrient metabolism and nitrogen
147 cycling (*napG, napH, narG, narH, narI, nrfA, narJ, nirB, nirD, narK, napC*). In contrast,
148 genes associated with siderophore, iron transport, and iron homeostasis were
149 downregulated, including *fiu, cirA, fepA, fyuA, efeO, efeU, efeB, fhuE, entD, entC, entF,*
150 *chuA, chuS, chuT*.

151 Gene Ontology (GO) term analysis reflected this multifaceted recipient response, with
152 significant enrichment in categories related to stress adaptation, respiratory activity, and
153 metabolic reprogramming (Fig 1c).

154 By comparing the conjugation condition to the donor alone, we aimed to uncover the global
155 expression profile of RP4 across the entire conjugating population, recognizing that this
156 expression could originate from either donor or transconjugant cells. This analysis
157 revealed a striking upregulation of 47 genes encoded by pVS520, spanning key functional
158 categories including DNA mobilisation (MOB), mating pair formation (MPF), regulation and
159 replication, host-kill systems (*kil*), and other cellular processes (Fig 1d). These findings
160 confirm prior transcriptional studies of RP4 during *E. coli* conjugation (24), demonstrating
161 that that RP4 undergoes intense transcriptional activation during conjugation with this
162 species, with nearly all transcriptional units switched on.

163 **Capsule shields the recipient from transcriptional reprogramming during**
164 **conjugation**

165 To assess whether the recipient response to RP4 conjugation was conserved, we
166 repeated our experiment using *K. pneumoniae* B5055 as the recipient. This strain's
167 hypermucoid capsule also allowed us to investigate how recipient cell surface structures
168 influence the transcriptional landscape during conjugation. Capsules are known barriers
169 to conjugation (8), and prior to RNA-seq, we confirmed that the capsule of *K. pneumoniae*
170 B5055 significantly inhibited RP4 conjugation (supplementary Fig 2). Since this effect has

171 only been demonstrated in *Klebsiella spp in vitro*, we extended our analysis to
172 *Acinetobacter baumannii* AB5075 and *Pasteurella multocida* VP161, confirming that
173 capsule similarly impedes conjugation in these species (Supplementary Fig 2). This
174 represents the first *in vitro* evidence that capsules broadly inhibit conjugation across
175 multiple genera beyond *Klebsiella*.

176 To investigate how the capsule influences the transcriptional response to conjugation, we
177 compared gene expression profiles in wild-type and acapsular *K. pneumoniae* recipients.
178 In the wild-type strain, only 10 genes were differentially expressed (including *carB, carA,*
179 *lysS, clbS, glnH,* 08025*, glnP,* and several uncharacterized loci: 08030, 08050, 08045*)*
180 (Fig 2a). These genes were associated with pathways such as sucrose catabolism, L-
181 arginine biosynthesis and nucleotide biosynthesis (Fig 2b).

182 However, when the acapsular mutant B5055Δ*wzbc* was used as the recipient, the
183 transcriptional response expanded dramatically to 54 genes. This striking increase
184 demonstrates that the capsule not only acts as a physical barrier to conjugation but also
185 shields the recipient from widespread transcriptional reprogramming. By limiting
186 conjugation frequency, the capsule effectively insulates the host transcriptome from the
187 impact of plasmid acquisition.

188 Building on this observation, we further examined this transcriptional landscape in the
189 absence of capsule. *K. pneumoniae* B5055Δ*wzbc* exhibited upregulation of stress
190 adaptation genes shared with *E. coli* (e.g. *cspD*, *nhaA*), as well as responses unique to
191 this strain (*loiP*, *ychH, hcp*). We also observed broad changes in genes involved in
192 carbohydrate transport (*araH, fucP, galP, manY, manZ, manX, bglF*), catabolism (*treC,*
193 *fruK pck, bglB, opbG*), and transmembrane transport (*psuT, sdaC, ompC, ttdT, nhaA,*
194 *yebQ, malE, gntT, ompW*).

195 Consistent with the *E. coli* response, genes linked to anaerobic growth (*ompW*, *ttdT*) and
196 anaerobic respiration (*fdnG, fdhF, narG*) were also activated. GO term analysis highlighted
197 enrichment in mixed stress responses and altered carbohydrate transport and metabolism
198 (Fig 2b). Using BLAST, we identified 13 homologous genes shared between the two
199 recipient species (*ysab, galP, ypfG, ypeC, ompW, narG, cspG, citT, nhaA,*

200 ACPEGL_23855*, ytjA*, *csgD* and *ompF*), indicating that approximately 10% of the
201 transcriptional response to RP4 is conserved.

202 **Capsules block conjugation by preventing donor cell activation and cell-to-cell**
203 **contact**

204 Capsules are potent inhibitors of bacterial conjugation, widely believed to block essential
205 donor-recipient contact, yet this mechanism has not been directly demonstrated. Before
206 examining their role in physical contact, we first asked whether capsules influence the
207 activation of RP4-encoded genes during conjugation. To address this, we re-analysed our
208 transcriptomic dataset comparing wild-type *K. pneumoniae* and its acapsular mutant
209 B5055Δ*wzbc*. When the recipient was encapsulated, no RP4 genes were activated (Fig
210 2d). In contrast, conjugation with the acapsular mutant triggered expression of 27 genes.
211 Notably, this was fewer than the number activated during conjugation with *E. coli*,
212 suggesting that RP4 gene expression is shaped by the specific recipient species.

213 To determine whether RP4 gene activation originated from the donor or transconjugant
214 cells, we employed a donor-specific fluorescent reporter assay targeting the relaxase
215 promoter. By using rifampicin to selectively silence recipient transcription, taking
216 advantage of donor rifampicin resistance, we confirmed that relaxase operon activation
217 occurred exclusively in donor cells. Crucially, this activation was blocked when the
218 recipient was encapsulated (Supplementary Fig 3).

219 These findings reveal that the capsule prevents the donor from sensing the recipient,
220 thereby suppressing transcriptional activation of RP4. This highlights a previously
221 unrecognized role of the capsule in modulating donor behavior during conjugation.

222 To uncover the mechanism by which capsule inhibits conjugation, we performed imaging
223 studies to directly visualize donor-recipient interactions in the presence and absence of
224 capsule. Transmission and scanning electron microscopy revealed that the capsule of
225 *K. pneumoniae* physically obstructs direct outer membrane contact between donor and
226 recipient cells (Fig 2e, top panels). In contrast, when the capsule was absent, intimate
227 membrane-to-membrane contact was readily observed (Fig 2e, bottom panels), consistent
228 with conditions permissive for conjugation. Unexpectedly, these imaging studies also

229 revealed substantial heterogeneity in capsule thickness and architecture at the single cell
230 level, a phenomenon explored further in a subsequent section (See Fig 3).

231 To directly test whether capsule-mediated inhibition of cell-to-cell contact blocks
232 conjugation, we performed fluorescence microscopy on agarose pad conjugation assays
233 (Fig 2f). We used an RP4-mobilisable plasmid encoding GFP to track plasmid transfer into
234 recipient cells labelled with BFP on a non-mobilizable plasmid. In conjugations with
235 acapsular mutant B5055Δ*wzbc*, 70% of donor-contacting recipient cells successfully
236 acquired the plasmid (369 transconjugants from 527 mating pairs; Fig 2f, right panel). In
237 stark contrast, only 0.58% of donor-contacting wild-type recipient cells formed
238 transconjugants (2 of 345 mating pairs), and overall mating pair formation was reduced
239 due to capsule-mediated inhibition of direct contact (Fig 2f, left panel). Notably, wild-type
240 *K. pneumoniae* B5055 cells also showed limited contact with each other, indicating that
241 the capsule restricts both intracellular and intercellular interactions.

242 Together, these results demonstrate that the capsule prevents donor recognition of the
243 recipient by physically blocking cell-to-cell contact, thereby suppressing conjugation.

244 **RP4 overcomes capsule-mediated conjugation barriers by exploiting capsule**
245 **thickness and expression variability**

246 During earlier imaging experiments, we observed striking variability in *K. pneumoniae*
247 capsular thickness at the single-cell level, prompting a more detailed analysis using SEM
248 and TEM (Fig 3).

249 SEM revealed that the capsule forms a complex cell surface matrix, often connecting
250 adjacent cells *via* thick, filamentous projections ranging from 0.5 μm to 4 μm in length.
251 These structures were present in 86% of cells examined (581/676), while a minority
252 displayed smooth, unstructured surfaces (Fig 3a).

253 TEM further showed that the capsule appears as a diffuse, often non-uniform layer, with
254 substantial variation in thickness between individual cells (Fig 3b-c). Quantification of total
255 capsule diameter across biological replicates revealed a wide range, from 132.8 nm to
256 678.8 nm, with a mean of 287 nm (Fig 3d). Surprisingly, even under identical growth and

257 processing conditions, capsule thickness varied significantly between replicates, with
258 mean values of 420.2 nm, 192.7 nm, and 263.3 nm, respectively (Fig 3d).

259 These findings demonstrate that *K. pneumoniae* exhibits pronounced phenotypic
260 heterogeneity in capsule architecture, even within clonal populations, highlighting a
261 potential vulnerability that RP4 may exploit to bypass capsule-mediated conjugation
262 barriers.

263 To determine whether variability in recipient capsule thickness enables rare conjugation
264 events in wild-type *K. pneumoniae*, we investigated whether thinner-capsule cells were
265 responsible for the small number of transconjugants observed. Since capsule blocks
266 conjugation by preventing close donor-recipient contact (Fig 2g-h), we hypothesized that
267 cells with thinner capsules might permit tighter membrane interactions, allowing plasmid
268 transfer to occur. To test this, we conducted further experiments to directly link capsule
269 heterogeneity with conjugation efficiency.

270 Supporting this hypothesis, both TEM and SEM imaging revealed that B5055 recipient
271 cells with thinner capsules formed significantly closer associations with donor cells
272 compared to those with thicker capsules (Fig 3 e-f). Quantitative analysis confirmed a
273 strong correlation between capsule thickness and the physical distance separating donor
274 and recipient outer membranes (Fig 3g, $R2=0.72$, $N=47$, F test $P<0.0001$), indicating that
275 thicker capsules physically increase intercellular spacing and reduce the likelihood of
276 conjugation.

277 Crucially, live-cell fluorescence microscopy showed that transconjugants arose
278 specifically from recipient cells capable of forming intimate contact with donors (Fig 3h).
279 These transconjugant cells appeared in tightly packed clusters and displayed a
280 morphology strikingly similar to the acapsular B5055Δ*wzbc* mutants (Fig 3h, inset),
281 consistent with them being thin-capsulated.

282 Together, these findings demonstrate that natural heterogeneity in capsule thickness
283 enables a subpopulation of recipient cells to bypass the capsule barrier, facilitating rare
284 but successful conjugation events.

285 Given the observed variability in capsule thickness across identically treated replicates
286 (Fig 3d), we hypothesized that this heterogeneity could occasionally permit higher
287 conjugation frequencies in the wild-type B5055 *K. pneumoniae* recipient. To test this, we
288 conducted 19 independent conjugation experiments, anticipating that natural fluctuations
289 in capsule thickness between replicates would influence conjugation efficiency. In 4 of
290 these experiments, we observed a markedly elevated mean transfer frequency of $4.2 \times 10^{-}$
291 ^{2} (Fig 4A), approximately ~50-fold higher than the median across all replicates, yet still 20-
292 fold lower than that observed with the acapsular B5055Δ*wzbc* mutant (Fig 4a). This
293 suggests that while capsule was still present, its barrier function was partially
294 compromised. Importantly, the resulting transconjugants remained mucoid and string-test
295 positive, confirming they were not spontaneous capsule-deficient mutants.

296 These findings indicate that stochastic variation in capsule expression can transiently
297 weaken its barrier function, enabling rare but enhanced conjugation events in otherwise
298 encapsulated populations.

299 To investigate the molecular basis of elevated conjugation in wild-type *K. pneumoniae*
300 replicates, we performed RNA-seq to compare RP4 conjugation events and recipient
301 capsule biosynthesis activity between high-frequency and low-frequency conjugation
302 events. In high frequency conjugations, RP4 gene expression resembled that observed in
303 the acapsular B5055Δ*wzbc* mutant (See Fig 2d), characterized by strong upregulation of
304 DNA mobilization genes, but not mating pair formation genes (Fig 4b).

305 Strikingly, these samples also showed markedly reduced expression of key capsule
306 biosynthesis genes under the control of the P*wzi* promoter (Fig 4c). Beyond *wzi*,13
307 additional capsule-associated genes (25) were differentially expressed, including the
308 master capsule synthesis regulator *kvrA* (26), and a suite of regulatory and structural
309 genes, such as *hha, ompR, pitA, miaA, arnD, ackA, wabH, rcsF, wabN, wcaG, fis, rfaH*
310 and *mlaF* (Fig 4d). Many other genes with diverse function were also differentially
311 expressed, suggesting a broader physiological shift in these high-frequency conjugation
312 conditions.

313 Together, these data reveal that reduced capsule gene expression underlies the increased
314 conjugation efficiency in certain wild-type replicates, reinforcing the role of capsule as a
315 dynamic and regulatable barrier to horizontal gene transfer.

316 Finally, to assess how variation in capsule serotype influences conjugation, we examined
317 the impact of different hypermucoid capsule types on RP4 transfer efficiency. Conjugation
318 with a hypermucoid K1 recipient resulted in a dramatic 31-fold reduction in transfer
319 frequency compared to its acapsular counterpart. In contrast, two hypermucoid K5
320 recipients showed more modest reductions of 3.3 and 2.2-fold, relative to their respective
321 wild-type controls. These findings demonstrate that while capsule consistently acts as a
322 barrier to conjugation, the magnitude of its inhibitory effect varies by serotype and is
323 independent of if the serotype is hypermucoid. This highlights that both dynamic capsular
324 thickness and serotype-specific properties govern conjugation efficiency through
325 mechanisms that are partially independent of capsular serotype.

326 Discussion

327 We investigated how recipient species and surface structures shape the early
328 transcriptional response and ultimate success of broad host range plasmid conjugation.
329 Our transcriptomic analyses revealed that plasmid acquisition is a highly transcriptionally
330 active process, triggering non-SOS stress responses and metabolic reprogramming in
331 recipient cells. Notably, we found that the bacterial capsule acts as a protective barrier,
332 shielding recipients from this transcriptional upheaval by physically blocking donor-
333 recipient contact and thereby preventing donor activation.

334 We further demonstrated that this inhibitory effect is not unique to *K. pneumoniae* since
335 capsules from *A. baumannii and P. multocida* also suppressed conjugation, establishing
336 capsules as broad-spectrum barriers to horizontal gene transfer. Strikingly, we discovered
337 that the capsule is not an absolute barrier. RP4 can exploit natural heterogeneity in
338 capsule thickness at the single-cell level to bypass this defense, enabling sporadic but
339 successful plasmid transfer into otherwise resistant populations.

340 Together, our findings provide a unified framework for understanding how recipient identity
341 and surface structure variability govern the transcriptional landscape and efficiency of

342 conjugation. This work offers new insights into how broad host range plasmids overcome
343 physical barriers to disseminate across diverse bacterial species.

344 A key finding of this study is that conjugation induces a far more extensive transcriptional
345 response than previously appreciated, extending well beyond the canonical SOS
346 response (27). Across both *E. coli* and *K. pneumoniae*, conjugation triggered broad non-
347 SOS stress responses and widespread reprogramming of respiratory, metabolic,
348 substrate transport, and other pathways. This likely reflects the substantial energetic and
349 homeostatic burden associated with establishing a new plasmid, consistent with the
350 commonly observed growth defects in newly formed RP4 transconjugants (28).

351 Despite species-specific differences, approximately 10% of the recipient transcriptional
352 response was shared between *E. coli* and *K. pneumoniae*. Notably, two conserved genes,
353 *ompW* and *nhaA*, have previously been shown to influence the conjugation efficiency of
354 multiple plasmids, including R388 and F-like plasmids (7, 29). OmpW, typically expressed
355 during the transition to anaerobic respiration (30), is targeted by mating pair stabilization
356 proteins during conjugation (7). NhaA, a key regulator of sodium ion, pH, and osmotic
357 balance (31), also contributes to cell envelope integrity (32), suggesting a protective role
358 against conjugation-induced envelope stress.

359 Importantly, this transcriptional upheaval was largely absent in wild-type *K. pneumoniae*,
360 where capsule production effectively suppressed the recipient response. Although only a
361 small number of genes were differentially expressed in the encapsulated strain, GO-term
362 analysis still identified numerous redundant terms, a known limitation of this method (33).
363 In contrast, the broader and more diverse gene expression changes observed in *E. coli*
364 and the acapsular mutant yielded a wide array of non-redundant GO terms, reinforcing the
365 conclusion that capsule acts as a transcriptional shield during conjugation.

366 Capsules have long been implicated as barriers to conjugation (9, 34), but here we provide
367 the first direct visual evidence that they physically block the essential donor-recipient
368 contact required for mating pair formation. Our findings reveal that this physical barrier
369 has two critical consequences for conjugation. First, by preventing plasmid transfer, the
370 capsule acts as a protective shield for the recipient, insulating it from the extensive

371 transcriptional reprogramming and stress responses triggered by plasmid acquisition. We
372 propose that this shielding effect may confer a selective advantage in competitive
373 environments, where maintaining cellular homeostasis is crucial for survival.

374 Second, we show that the capsule effectively masks the recipient from the donor,
375 preventing the donor from initiating conjugation. Although the necessity of direct cell-to-
376 cell contact for conjugation has been recognized since the 1950s (35), the role of the
377 recipient during this contact has remained poorly defined. In the case of RP4, stable
378 donor-recipient contact is required for conjugative junction formation (36), yet previous
379 genetic screens in *E. coli* have failed to identify recipient genes essential for RP4-mediated
380 transfer (37).

381 By demonstrating that contact with a capsulated recipient is insufficient to trigger donor
382 activation, we provide compelling evidence that a recipient-encoded envelope factor,
383 obscured by the capsule, is required to initiate donor transcriptional activation. This aligns
384 with recent findings that R388 pilus expression is contact-dependent (38), but our data
385 suggest that, for RP4, it is the formation of the relaxosome, rather than pilus expression,
386 that is contingent on recipient recognition. Further, we show that contact with capsule is
387 not sufficient to trigger donor activation, showing that contact alone is not sufficient for
388 conjugation.

389 Unexpectedly, we found that the capsule is not an absolute barrier to conjugation, but
390 rather a leaky one, where natural variation in capsule thickness at the single-cell level
391 permits occasional RP4 transfer. Previous studies had indirectly linked capsule volume to
392 the degree of conjugation inhibition (8), but here we provide direct evidence that capsule
393 thickness precisely determines the physical distance between donor and recipient
394 membranes. This spatial separation in critical, as it governs the likelihood of successful
395 mating pair formation.

396 Capsular heterogeneity is well-documented across many bacterial species (39-42), and
397 our findings reveal a novel functional consequence of this variability: it modulates
398 horizontal gene transfer. In *K. pneumoniae*, capsule expression is regulated by complex
399 networks involving over 70 genes (25, 43) and is largely non-phase-variable (25, 44, 45).

400 Our data suggest that the observed variation in capsular thickness is predominantly
401 stochastic, with no consistent pattern of expression across the population.

402 While the functional significance of single-cell heterogeneity in conjugation has only
403 recently begun to emerge (46, 47), our study uncovers a new dimension, specifically, that
404 dynamic, stochastic variation in recipient capsule thickness enables broad host range
405 plasmids like RP4 to breach an otherwise effective barrier and disseminate across
406 encapsulated bacterial populations.

407 In conclusion, our study reveals that conjugation is a transcriptionally demanding process
408 for recipient cells, extending well beyond the classical SOS response, and that this
409 response is shaped by both species identity and surface architecture. We demonstrate
410 that the bacterial capsule plays a dual role in modulating conjugation: it physically blocks
411 donor-recipient contact, thereby preventing donor activation, and it shields the recipient
412 from the transcriptional stress associated with plasmid acquisition. RP4 can exploit
413 natural, single-cell variation in capsule thickness to bypass this defense and successfully
414 transfer into encapsulated populations.

415 These findings have broad implications for understanding how conjugative plasmids,
416 carrying antibiotic resistance, virulence factors, and metabolic traits, navigate physical
417 barriers to spread across diverse bacterial species. Capsule heterogeneity emerges as a
418 critical factor influencing the success of horizontal gene transfer, with important
419 consequences for microbial evolution and the dissemination of clinically relevant traits.

420 Materials and Methods

421 Bacterial strains, plasmids, and growth conditions

422 Table 1 lists the bacterial strains and plasmids used in this work. For routine growth, *E.*
423 *coli* and *K. pneumoniae* strains were cultured in low-salt LB at 37°C shaking in liquid at
424 200 rpm or on solid media. Media was supplemented with antibiotics where necessary:
425 Ampicillin (100 µg ml^{-1}), rifampicin (150 µg ml^{-1}), erythromycin (150 µg/ml), spectinomycin
426 (50 µg/ml) and tetracycline (10 µg ml^{-1}).

427 Strain and plasmid construction

428 Prior to use as recipients, wildtype and Δ*wzbc K. pneumoniae*, along with *E. coli* DLL7555,
429 were electroporated with the low copy number vector pWSK29 to provide an ampicillin counter
430 selection maker for conjugation. Fluorescent reporter plasmids were made as follows.
431 *GFPmut3* or *mTagBFP2* were fused to a synthetic *em7* promoter (48) and synthesised as
432 gBlocks (IDT). These were cloned into the XbaI and BamHI site of pMMB67EH or pSU18
433 respectively through restriction digestion cloning. pWSK29P*traJ*GFPx3 was similarly
434 constructed, except that three translationally coupled copies of *mGreenLantern* were fused to
435 a 367 bp region upstream of the *traJ* start codon. Each *mGreenLantern* subunit was
436 independently codon optimised until each shared < 80% sequence homology.

437 **Conjugation assays**

438 Overnight liquid cultures of donor and recipient were diluted 1:50 in fresh LB and grown
439 for 4 hours before being washed once in PBS and normalized to an OD_{600} 1.0. 500 µl of
440 donor and recipient culture was passed through a 0.44 µm nitrocellulose membrane filter
441 (Whattman) and incubated on LB agar at 37°C for 15 minutes before extraction in 2 ml of
442 PBS by vigorous vortexing. 15 minutes was chosen as a timepoint to prevent secondary
443 transmission of plasmid RP4, and to minimize growth of the recipient which can skew
444 transfer frequencies. For routine assays, recipient and transconjugant CFU/ml were
445 quantified by plating onto ampicillin, and ampicillin + tetracycline respectively. For *A.*
446 *baumannii*, transconjugants were quantified on ampicillin + erythromycin using mobilizable
447 plasmid RSF1010 *erm* as a surrogate for RP4 transfer. For *P. multocida,* kanamycin +
448 spectinomycin using mobilizable plasmid pAL99S-*oriT* as a surrogate for RP4 transfer was
449 performed. Conjugation frequency was calculated as the transconjugant CFU/ml divided
450 by recipient CFU/ml.

451 **RNA extraction and sequencing**

452 Conjugations were fixed after 15 minutes of incubation by vortexing mating filters in
453 RNAprotect (Qiagen). Fixed samples were pelleted at 13,300 RPM for 5 minutes, the
454 RNAprotect decanted and samples stored at -80°C for later processing. RNA was
455 extracted from the DLL7555 samples using an RNeasy RNA extraction kit (Qiagen) as per
456 the manufacturer's instructions with an on-column DNase treatment (Qiagen). Due to its
457 thick capsule, RNA from *K. pneumoniae* was isolated with hot-phenol as previously
458 described (49) and further purified using an RNeasy kit with on column-DNase treatment.

459 RNA from DLL7555-related experiments was sequenced at the MHTP Medical Genomics
460 Facility at the Monash Translational Facility. Samples were quality checked by Bioanalyzer
461 (Agilent), and libraries generated using the Illumina stranded total RNA-seq protocol with
462 ribosomal RNA depletion performed using the bacterial Ribo-Zero rRNA removal kit
463 (Illumina). Sequencing was performed on an Illumina NextSeq550 on high output mode
464 with chemistry version 2.5, using the Illumina protocol 15046563 version 2. RNA from *K.*
465 *pneumoniae* related experiments was sequenced at Micromon Genomics. Samples were
466 quality checked by Fragment Analyzer (AATI) and RNA library construction performed
467 using MGI Tech MGIEasy RNA Directional Library Prep Kit V2 (1000006386). Ribosomal
468 RNA was depleted using the rRNA depletion kit bacteria (NEB). Resulting libraries were
469 sequenced on an MGIEasy MGISEQ2000RS using V2 chemistry. For all experiments,
470 samples were sequenced to a depth that would ensure least 10 million reads per isolate
471 in the sample.

472 **Transcriptomic analysis**

473 Prior to analysis, we assessed the suitability of our two genetically distant *E. coli* donor
474 and recipient strains for RNA-seq analysis. Genetic variation between the donor and
475 recipient was assessed using snippy version 4.6 (50) which detected >75,000 genetic
476 variants including >68,000 SNPs which were equally distributed across the recipient
477 genome (Supplementary Fig 4). This number was in line with previous single species co-
478 culture RNA-seq experiments (51). Although the two strains were sufficiently genetically
479 distinct, 53 genes that were identical between DLL7555 and HB101 were excluded from
480 the final analysis. RNA reads were aligned against a concatenated sequence of the donor
481 (accession, CP184671.1), recipient (DLL7555, accession CP186931.1 or B5055,
482 assembly GCF_024138975.1), and pVS520 sequences (CP184672.1). The sequence for
483 HB101 (Rif^S version of LT101) was used as the donor sequence owing to its availability.
484 Read alignment was performed with subread version v1.5.1 (52) against the concatenated
485 sequence which discarded reads of ambiguous donor/recipient origin. >99.8% of donor
486 originating reads were filtered by this strategy for both B5055 and DLL755 matings, which
487 was assessed by alignment of RNA isolated from the donor only condition against the
488 concatenated sequence. Read counting and assignment were performed via
489 FeatureCounts (53). Differential gene expression was analysed with the Voom/Limma

490 method in Degust v4.1 (https://drpowell.github.io/degust/) with a minimum of 3 counts per
491 million reads across 3 samples. At this stage, an additional 5 genes were subsequently
492 excluded from the DLL7555 analysis due to the detection of donor originating reads which
493 were not successfully filtered earlier. Genes were considered differentially expressed if
494 they had a Log2 fold change ≥ 0.585, a P value ≤ 0.05, and an FDR ≤ 0.05. GO term
495 analysis was performed using the TopGO R package v2.58 (54), with the weight_01
496 algorithm using raw P-values due to the structured dependency of GO terms as per the
497 package guidelines. eggNOG mapper v2.1.8 (55) was used to assign GO-terms to the
498 GenBank recipient proteomes. Gene and pathway functions were also assessed using the
499 ecocyc database (56). Heatmaps and GO term plots were generated using ggplot2 v3.5.2
500 (57) and the geneviewer package version 0.1.1 (https://github.com/nvelden/geneviewer).

501 **Scanning and Transmission Electron Microscopy**

502 SEM was performed on *K. pneumoniae* cells during conjugation, or in stationary phase
503 when capsule is highly expressed (25). 500 µl of cells were collected onto a 0.4 µm
504 polycarbonate membrane, and the capsular ultrastructure preserved by lysine acetate,
505 ruthenium red and osmium (LRR) fixation (58), followed by graduated dehydration in
506 ethanol, critical point drying, and gold sputter coating as previously described (59).
507 Samples were imaged on a field emission NovaSEM 450 SEM with an acceleration
508 voltage of 10 kV in secondary electron mode with a working distance of ~4.5mm. Images
509 were taken under immersion mode through the lens detector.

510 For TEM imaging, cells were collected on polycarbonate membranes and prepared with
511 LRR fixation as for SEM. Fixed membranes were then cut into small rectangles no longer
512 than 1 mm cubed, dehydrated and then infiltrated with Epon resin (60). Each membrane
513 was placed on a glass slide cell-side up, and a BEEM® capsule containing 100% resin
514 positioned over the flat membrane before polymerisation at 60°C for 48 hours. The resin-
515 filled BEEM® capsule and slide were cooled in liquid nitrogen and then immediately
516 separated, leaving the flat membrane with cells in a longitudinal orientation on the surface
517 of the resin block. Cells were ultrathin sectioned using a Leica UC7 ultramicrotome and
518 Diatome diamond knife and then contrasted with uranyl acetate and lead citrate. Cells
519 were imaged on a JEOL JEM-1400 Plus TEM at 80 KeV, equipped with a high sensitivity

520 bottom mount CMOS 'Flash' camera. Total capsule diameter was measured from the
521 average of 5 total cell widths from which the cell body width was subtracted, as described
522 previously (61).

523 **Fluorescent Microscopy and Image analysis**

524 Conjugation was analysed by fluorescent microscopy by inoculation of 1 µl of OD_{600} 0.1
525 recipient and donor onto LB 1% agarose pads. Pads were incubated in parafilm sealed 25
526 mm fluorodish chamber (WPI) for 2 hours at 37°C. Small strips of moist KimWipe® were
527 included in the chamber to prevent pad dehydration. Images were acquired using a
528 63x/1.30 oil objective on a Leica DMI-8 widefield microscope equipped with a Lecia K8
529 sCMOS monochromatic camera using Lecia LasX software. Mating pair productivity was
530 assessed by counting transconjugants that were in direct contact with a donor and dividing
531 that by the total number of recipients in contact with a donor

532 **Fluorescent reporter assays**

533 Fluorescent measurements were taken on a Tecan infinite pro 200 plate reader. For
534 measurement of P*traJ*, 15 µl of *K. pneumoniae* was inoculated onto a 200 µl LB 1%
535 agarose pad with rifampicin in a 96-well special optics microtiter plate (Corning). After 5
536 minutes of incubation and air drying, 15 µl of donor culture was spotted on top and
537 immediately afterwards the OD600 and fluorescent intensity (488 nm / 520 nm) were
538 measured in 5-minute intervals at 37°C. Fluorescent intensity was then normalised to
539 OD600 and analysed as change over time by calculating fold-change against the 0-time
540 point value.

541 **Acknowledgments:** We would like to acknowledge Dr Francesca Short for providing
542 strains and protocols for RNA isolation, and Dr Tom Smallman and Prof John Boyce for
543 providing strains. The authors acknowledge use of the facilities and the assistance of Alex
544 Fulcher from Monash Micro Imaging. The authors acknowledge the use of instruments
545 and assistance at the Monash Ramaciotti Centre for Cryo-Electron Microscopy, a Node of
546 Microscopy Australia. The authors acknowledge the MHTP Medical Genomics Facility for
547 assistance with RNA sequencing.

Funding: This work was supported by the Australian Research Council Grant DP250103521, and Australian Research Council Laureate Fellowship FL210100258 awarded to D.L., and funding for Y.H. Gan from the National Medical Research Council, grant number OFIRG20NOV-0045.

Data availability: Transcriptomic data have been submitted to the NCBI SRA under the bioproject accession PRJNA1286074

556 ## References

557 1. S. Redondo-Salvo *et al.*, Pathways for horizontal gene transfer in bacteria revealed by a
558 global map of their plasmids. *Nat Commun* **11**, 3602 (2020).
559 2. S. Castañeda-Barba, E. M. Top, T. Stalder, Plasmids, a molecular cornerstone of
560 antimicrobial resistance in the One Health era. *Nature Reviews Microbiology* **22**, 18-32
561 (2024).
562 3. W. Matlock *et al.*, Enterobacterales plasmid sharing amongst human bloodstream
563 infections, livestock, wastewater, and waterway niches in Oxfordshire, UK. *Elife* **12** (2023).
564 4. C. Virolle, K. Goldlust, S. Djermoun, S. Bigot, C. Lesterlin, Plasmid Transfer by Conjugation
565 in Gram-Negative Bacteria: From the Cellular to the Community Level. *Genes (Basel)* **11**
566 (2020).
567 5. L. Toribio-Celestino, A. San Millan, Plasmid–bacteria associations in the clinical
568 context. *Trends in Microbiology* **33**, 937-947 (2025).
569 6. M. P. Garcillán-Barcia, F. de la Cruz, E. P. Rocha, The extended mobility of plasmids.
570 *Nucleic Acids Research* **53**, gkaf652 (2025).
571 7. W. W. Low *et al.*, Mating pair stabilization mediates bacterial conjugation species
572 specificity. *Nature Microbiology* **7**, 1016-1027 (2022).
573 8. M. Haudiquet *et al.*, Capsules and their traits shape phage susceptibility and plasmid
574 conjugation efficiency. *Nature Communications* **15**, 2032 (2024).
575 9. M. Yong *et al.*, Dominant Carbapenemase-Encoding Plasmids in Clinical Enterobacterales
576 Isolates and Hypervirulent Klebsiella pneumoniae, Singapore. *Emerg Infect Dis* **28**, 1578-
577 1588 (2022).
578 10. K. Billane, E. Harrison, D. Cameron, M. A. Brockhurst, Why do plasmids manipulate the
579 expression of bacterial phenotypes? *Philosophical Transactions of the Royal Society B:*
580 *Biological Sciences* **377**, 20200461 (2022).
581 11. H. Lee, K. S. Ko, Effect of multiple, compatible plasmids on the fitness of the bacterial host
582 by inducing transcriptional changes. *Journal of Antimicrobial Chemotherapy* **76**, 2528-
583 2537 (2021).
584 12. C. Huang *et al.*, Comparative Analysis of Transcriptome and Proteome Revealed the
585 Common Metabolic Pathways Induced by Prevalent ESBL Plasmids in Escherichia coli.
586 *International Journal of Molecular Sciences* **24**, 14009 (2023).
587 13. A. San Millan, M. Toll-Riera, Q. Qi, R. C. MacLean, Interactions between horizontally
588 acquired genes create a fitness cost in Pseudomonas aeruginosa. *Nature Communications*
589 **6**, 6845 (2015).
590 14. K. Schaufler *et al.*, Carriage of Extended-Spectrum Beta-Lactamase-Plasmids Does Not
591 Reduce Fitness but Enhances Virulence in Some Strains of Pandemic E. coli Lineages. *Front*
592 *Microbiol* **7**, 336 (2016).
593 15. Z. Baharoglu, D. Bikard, D. Mazel, Conjugative DNA Transfer Induces the Bacterial SOS
594 Response and Promotes Antibiotic Resistance Development through Integron Activation.
595 *PLOS Genetics* **6**, e1001165 (2010).
596 16. C. Zhao *et al.*, Horizontal transfer of the multidrug resistance plasmid RP4 inhibits
597 ammonia nitrogen removal dominated by ammonia-oxidizing bacteria. *Water Research*
598 **217**, 118434 (2022).

599 17. Z. Yu, Y. Wang, J. Lu, P. L. Bond, J. Guo, Nonnutritive sweeteners can promote the
600 dissemination of antibiotic resistance through conjugative gene transfer. *Isme j* **15**, 2117-
601 2130 (2021).
602 18. Y. Wu *et al.*, Biochar Effectively Inhibits the Horizontal Transfer of Antibiotic Resistance
603 Genes via Restraining the Energy Supply for Conjugative Plasmid Transfer. *Environ Sci*
604 *Technol* **56**, 12573-12583 (2022).
605 19. L. González-Montes, I. Del Campo, M. P. Garcillán-Barcia, F. de la Cruz, G. Moncalián,
606 ArdC, a ssDNA-binding protein with a metalloprotease domain, overpasses the recipient
607 hsdRMS restriction system broadening conjugation host range. *PLoS Genet* **16**, e1008750
608 (2020).
609 20. C. Coluzzi, E. P. C. Rocha, The Spread of Antibiotic Resistance Is Driven by Plasmids Among
610 the Fastest Evolving and of Broadest Host Range. *Molecular Biology and Evolution* **42**
611 (2025).
612 21. O. Rendueles, J. A. M. de Sousa, A. Bernheim, M. Touchon, E. P. C. Rocha, Genetic
613 exchanges are more frequent in bacteria encoding capsules. *PLoS Genet* **14**, e1007862
614 (2018).
615 22. T. D. Lawley, G. S. Gordon, A. Wright, D. E. Taylor, Bacterial conjugative transfer:
616 visualization of successful mating pairs and plasmid establishment in live Escherichia coli.
617 *Molecular Microbiology* **44**, 947-956 (2002).
618 23. J. M. Ghigo, Natural conjugative plasmids induce bacterial biofilm development. *Nature*
619 **412**, 442-445 (2001).
620 24. M. Miyakoshi, Y. Ohtsubo, Y. Nagata, M. Tsuda, Transcriptome Analysis of Zygotic
621 Induction During Conjugative Transfer of Plasmid RP4. *Frontiers in Microbiology* **Volume**
622 **11 - 2020** (2020).
623 25. M. J. Dorman, T. Feltwell, D. A. Goulding, J. Parkhill, F. L. Short, The Capsule Regulatory
624 Network of Klebsiella pneumoniae Defined by density-TraDISort. *mBio* **9** (2018).
625 26. M. Palacios *et al.*, Identification of Two Regulators of Virulence That Are Conserved in
626 Klebsiella pneumoniae Classical and Hypervirulent Strains. *mBio* **9** (2018).
627 27. H. D. Curtsinger, S. Martínez-Absalón, Y. Liu, A. J. Lopatkin, The metabolic burden
628 associated with plasmid acquisition: An assessment of the unrecognized benefits to host
629 cells. *Bioessays* 10.1002/bies.202400164, e2400164 (2024).
630 28. H. Prensky, A. Gomez-Simmonds, A. C. Uhlemann, A. J. Lopatkin, Conjugation dynamics
631 depend on both the plasmid acquisition cost and the fitness cost. *Molecular Systems*
632 *Biology* **17**, e9913 (2021).
633 29. D. Pérez-Mendoza, F. de la Cruz, Escherichia coli genes affecting recipient ability in
634 plasmid conjugation: Are there any? *BMC Genomics* **10**, 71 (2009).
635 30. M. Xiao, Y. Lai, J. Sun, G. Chen, A. Yan, Transcriptional Regulation of the Outer Membrane
636 Porin Gene ompW Reveals its Physiological Role during the Transition from the Aerobic
637 to the Anaerobic Lifestyle of Escherichia coli. *Front Microbiol* **7**, 799 (2016).
638 31. T. A. Krulwich, G. Sachs, E. Padan, Molecular aspects of bacterial pH sensing and
639 homeostasis. *Nat Rev Microbiol* **9**, 330-343 (2011).
640 32. Z. Mao *et al.*, NhaA facilitates the maintenance of bacterial envelope integrity and the
641 evasion of complement attack contributing to extraintestinal pathogenic Escherichia coli
642 virulence. *Infect Immun* **91**, e0003923 (2023).

643 33. R. Barriot, D. J. Sherman, I. Dutour, How to decide which are the most pertinent overly-
644 represented features during gene set enrichment analysis. *BMC Bioinformatics* **8**, 332
645 (2007).
646 34. M. Haudiquet, A. Buffet, O. Rendueles, E. P. C. Rocha, Interplay between the cell envelope
647 and mobile genetic elements shapes gene flow in populations of the nosocomial
648 pathogen Klebsiella pneumoniae. *PLOS Biology* **19**, e3001276 (2021).
649 35. B. D. Davis, Nonfiltrability of the agents of genetic recombination in Escherichia coli. *J*
650 *Bacteriol* **60**, 507-508 (1950).
651 36. A. L. Samuels, E. Lanka, J. E. Davies, Conjugative junctions in RP4-mediated mating of
652 Escherichia coli. *J Bacteriol* **182**, 2709-2715 (2000).
653 37. K. Moriguchi *et al.*, Targeting Antibiotic Resistance Genes Is a Better Approach to Block
654 Acquisition of Antibiotic Resistance Than Blocking Conjugal Transfer by Recipient Cells: A
655 Genome-Wide Screening in Escherichia coli. *Front Microbiol* **10**, 2939 (2019).
656 38. A. K. Vadakkepat *et al.*, Cryo-EM structure of the R388 plasmid conjugative pilus reveals
657 a helical polymer characterized by an unusual pilin/phospholipid binary complex.
658 *Structure* 10.1016/j.str.2024.06.009 (2024).
659 39. S. E. George *et al.*, Phenotypic heterogeneity and temporal expression of the capsular
660 polysaccharide in Staphylococcus aureus. *Molecular Microbiology* **98**, 1073-1088 (2015).
661 40. J. E. King, H. A. Aal Owaif, J. Jia, I. S. Roberts, Phenotypic Heterogeneity in Expression of
662 the K1 Polysaccharide Capsule of Uropathogenic Escherichia coli and Downregulation of
663 the Capsule Genes during Growth in Urine. *Infect Immun* **83**, 2605-2613 (2015).
664 41. L. M. Reyes Ruiz, C. L. Williams, R. Tamayo, Enhancing bacterial survival through
665 phenotypic heterogeneity. *PLOS Pathogens* **16**, e1008439 (2020).
666 42. A. Nucci *et al.*, Phenotypic heterogeneity of capsule production across opportunistic
667 pathogens. *mBio* **0**, e01807-01825 (2025).
668 43. K. A. Walker, V. L. Miller, The intersection of capsule gene expression, hypermucoviscosity
669 and hypervirulence in Klebsiella pneumoniae. *Current opinion in microbiology* **54**, 95-102
670 (2020).
671 44. M. A. Schembri, J. Blom, K. A. Krogfelt, P. Klemm, Capsule and fimbria interaction in
672 Klebsiella pneumoniae. *Infect Immun* **73**, 4626-4633 (2005).
673 45. D.-W. Wei *et al.*, Insertion sequences accelerate genomic convergence of multidrug
674 resistance and hypervirulence in Klebsiella pneumoniae via capsular phase variation.
675 *Genome Medicine* **17**, 45 (2025).
676 46. V. Cyriaque *et al.*, Single-cell RNA sequencing reveals plasmid constrains bacterial
677 population heterogeneity and identifies a non-conjugating subpopulation. *Nature*
678 *Communications* **15**, 5853 (2024).
679 47. R. J. B. Erickson *et al.*, Single-Cell Analysis Reveals that the Enterococcal Sex Pheromone
680 Response Results in Expression of Full-Length Conjugation Operon Transcripts in All
681 Induced Cells. *J Bacteriol* **202** (2020).
682 48. S. Zobel *et al.*, Tn7-Based Device for Calibrated Heterologous Gene Expression in
683 Pseudomonas putida. *ACS Synthetic Biology* **4**, 1341-1351 (2015).
684 49. N. R. Mattatall, K. E. Sanderson, Salmonella typhimurium LT2 possesses three distinct 23S
685 rRNA intervening sequences. *Journal of Bacteriology* **178**, 2272-2278 (1996).

686 50. T. Seemann, Snippy: rapid haploid variant calling and core SNP phylogeny. *GitHub.*
687 *Available at: github. com/tseemann/snippy* (2015).
688 51. T. A. Gray *et al.*, Intercellular communication and conjugation are mediated by ESX
689 secretion systems in mycobacteria. *Science* **354**, 347-350 (2016).
690 52. Y. Liao, G. K. Smyth, W. Shi, The Subread aligner: fast, accurate and scalable read mapping
691 by seed-and-vote. *Nucleic Acids Res* **41**, e108 (2013).
692 53. Y. Liao, G. K. Smyth, W. Shi, featureCounts: an efficient general purpose program for
693 assigning sequence reads to genomic features. *Bioinformatics* **30**, 923-930 (2014).
694 54. A. Alexa, J. Rahnenführer, Gene set enrichment analysis with topGO. *Bioconductor Improv*
695 **27**, 776 (2009).
696 55. C. P. Cantalapiedra, A. Hernández-Plaza, I. Letunic, P. Bork, J. Huerta-Cepas, eggNOG-
697 mapper v2: Functional Annotation, Orthology Assignments, and Domain Prediction at the
698 Metagenomic Scale. *Molecular Biology and Evolution* **38**, 5825-5829 (2021).
699 56. P. D. Karp *et al.*, The EcoCyc Database (2023). *EcoSal Plus* **11**, eesp-0002-2023 (2023).
700 57. H. Wickham, C. Sievert, *ggplot2: elegant graphics for data analysis* (springer New York,
701 2009), vol. 10.
702 58. S. Hammerschmidt, M. Rohde, "Electron Microscopy to Study the Fine Structure of the
703 Pneumococcal Cell" in Streptococcus pneumoniae: Methods and Protocols*,* F. Iovino, Ed.
704 (Springer New York, New York, NY, 2019), 10.1007/978-1-4939-9199-0_2, pp. 13-33.
705 59. T. R. Smallman, G. C. Williams, M. Harper, J. D. Boyce, Genome-Wide Investigation of
706 Pasteurella multocida Identifies the Stringent Response as a Negative Regulator of
707 Hyaluronic Acid Capsule Production. *Microbiology Spectrum* **10**, e00195-00122 (2022).
708 60. S. A. C. Jillian C Danne and Jillian C Danne, Rachel Templin, Joan Clark, Viola Oorschot,
709 Georg Ramm, Preparation of cells for transmission electron microscopy ultrastructural
710 analysis. *protocols.io* dx.doi.org/10.17504/protocols.io.j8nlk47ewg5r/v1 (2022).
711 61. T. Guess *et al.*, Size Matters: Measurement of Capsule Diameter in Cryptococcus
712 neoformans. *JoVE* doi:10.3791/57171, e57171 (2018).
713 62. B. M. Coffey, G. G. Anderson, Biofilm formation in the 96-well microtiter plate. *Methods*
714 *Mol Biol* **1149**, 631-641 (2014).
715 63. E. A. Palombo, K. Yusoff, V. A. Stanisich, V. Krishnapillai, N. S. Willetts, Cloning and genetic
716 analysis of tra cistrons of the Tra 2/Tra 3 region of plasmid RP1. *Plasmid* **22**, 59-69 (1989).
717 64. Y. Fu *et al.*, Mechanisms of blaIMP-4 dissemination across diverse carbapenem-resistant
718 clinical isolates. *Journal of Global Antimicrobial Resistance* **41**, 189-194 (2025).
719 65. M. M. C. Lam *et al.*, Population genomics of hypervirulent Klebsiella pneumoniae clonal-
720 group 23 reveals early emergence and rapid global dissemination. *Nature*
721 *Communications* **9**, 2703 (2018).
722 66. I. R. Lee *et al.*, Differential host susceptibility and bacterial virulence factors driving
723 Klebsiella liver abscess in an ethnically diverse population. *Scientific Reports* **6**, 29316
724 (2016).
725 67. A. C. Jacobs *et al.*, AB5075, a Highly Virulent Isolate of Acinetobacter baumannii, as a
726 Model Strain for the Evaluation of Pathogenesis and Antimicrobial Treatments. *mBio* **5**,
727 e01076-01014 (2014).
728 68. L. A. Gallagher *et al.*, Resources for Genetic and Genomic Analysis of Emerging Pathogen
729 Acinetobacter baumannii. *J Bacteriol* **197**, 2027-2035 (2015).

730 69. R. F. Wang, S. R. Kushner, Construction of versatile low-copy-number vectors for cloning,
731 sequencing and gene expression in Escherichia coli. *Gene* **100**, 195-199 (1991).
732 70. B. Bartolomé, Y. Jubete, E. Martínez, F. de la Cruz, Construction and properties of a family
733 of pACYC184-derived cloning vectors compatible with pBR322 and its derivatives. *Gene*
734 **102**, 75-78 (1991).
735 71. J. P. Fürste *et al.*, Molecular cloning of the plasmid RP4 primase region in a multi-host-
736 range tacP expression vector. *Gene* **48**, 119-131 (1986).

737

738

Figures and Tables

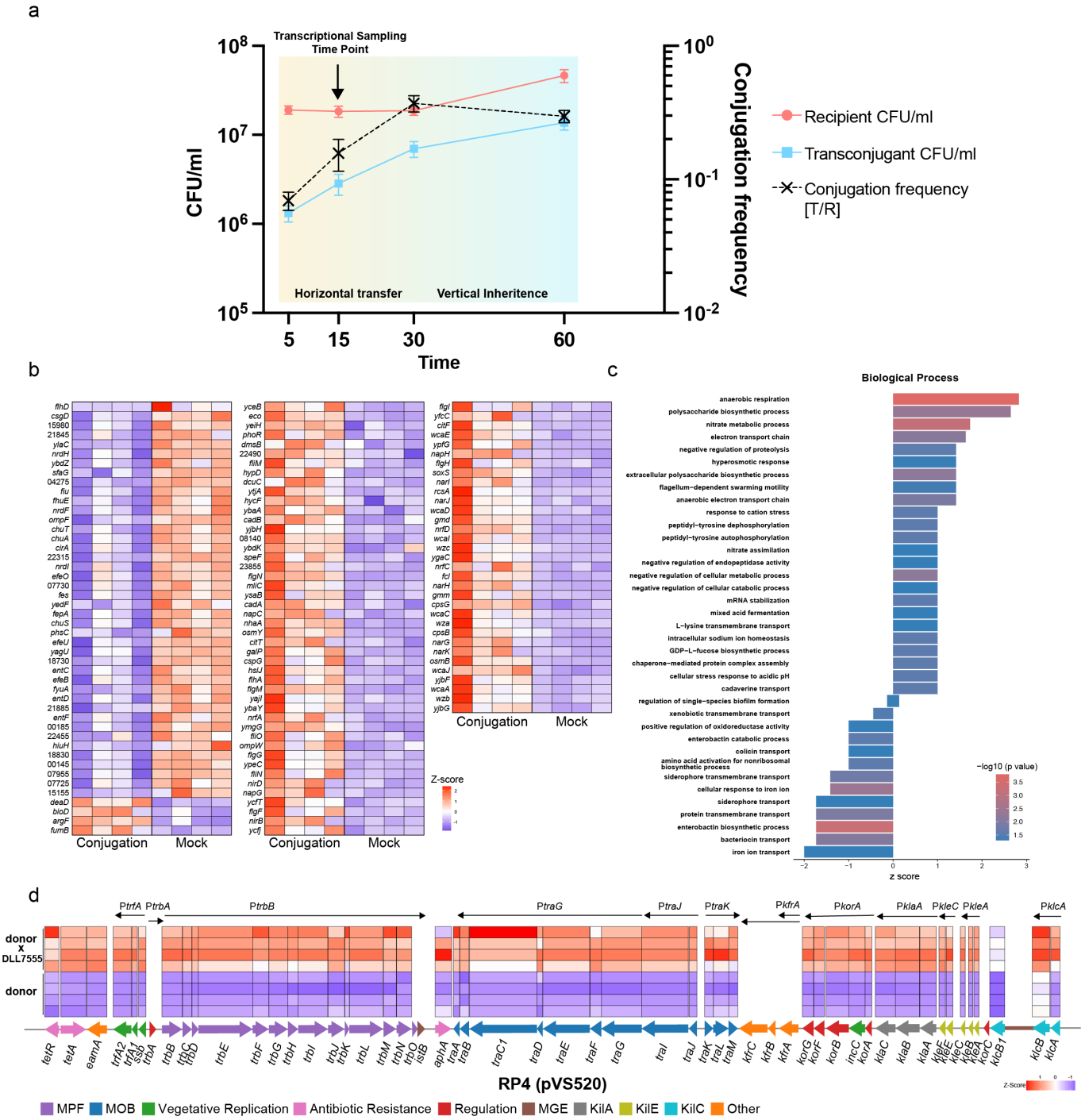
a
Transcriptional Sampling Time Point
Horizontal transfer
Vertical Inheritence
CFU/ml
Conjugation frequency
Time
Recipient CFU/ml
Transconjugant CFU/ml
Conjugation frequency [T/R]
b
Conjugation
Mock
Z-score
c
Biological Process
−log10 (p value)
z score
d
donor x DLL7555
donor
RP4 (pVS520)
MPF
MOB
Vegetative Replication
Antibiotic Resistance
Regulation
MGE
KilA
KilE
KilC
Other

741

742 **Figure 1. The transcriptional response of an *E. coli* recipient and plasmid RP4 during active**
743 **conjugation**. **a)** *E. coli* DLL7555 conjugation frequency over time shows that RP4 conjugation is
744 active at 15 minutes and completed by 30 minutes. Arrow indicates time for transcriptional
745 sampling. **b)** Differentially expressed DLL7555 genes during active RP4 conjugation. **c)** GO term
746 analysis of enriched genes with the R TopGo package with the weight_01 algorithm. **d)** Differential
747 expression of RP4-encoded genes during active conjugation with *E. coli* DLL7555. Numbers in *E.*
748 *coli* gene list represent locus tags trimmed of the prefix ACPEGL. Error bars = mean ± SD, N = 4.
749

750

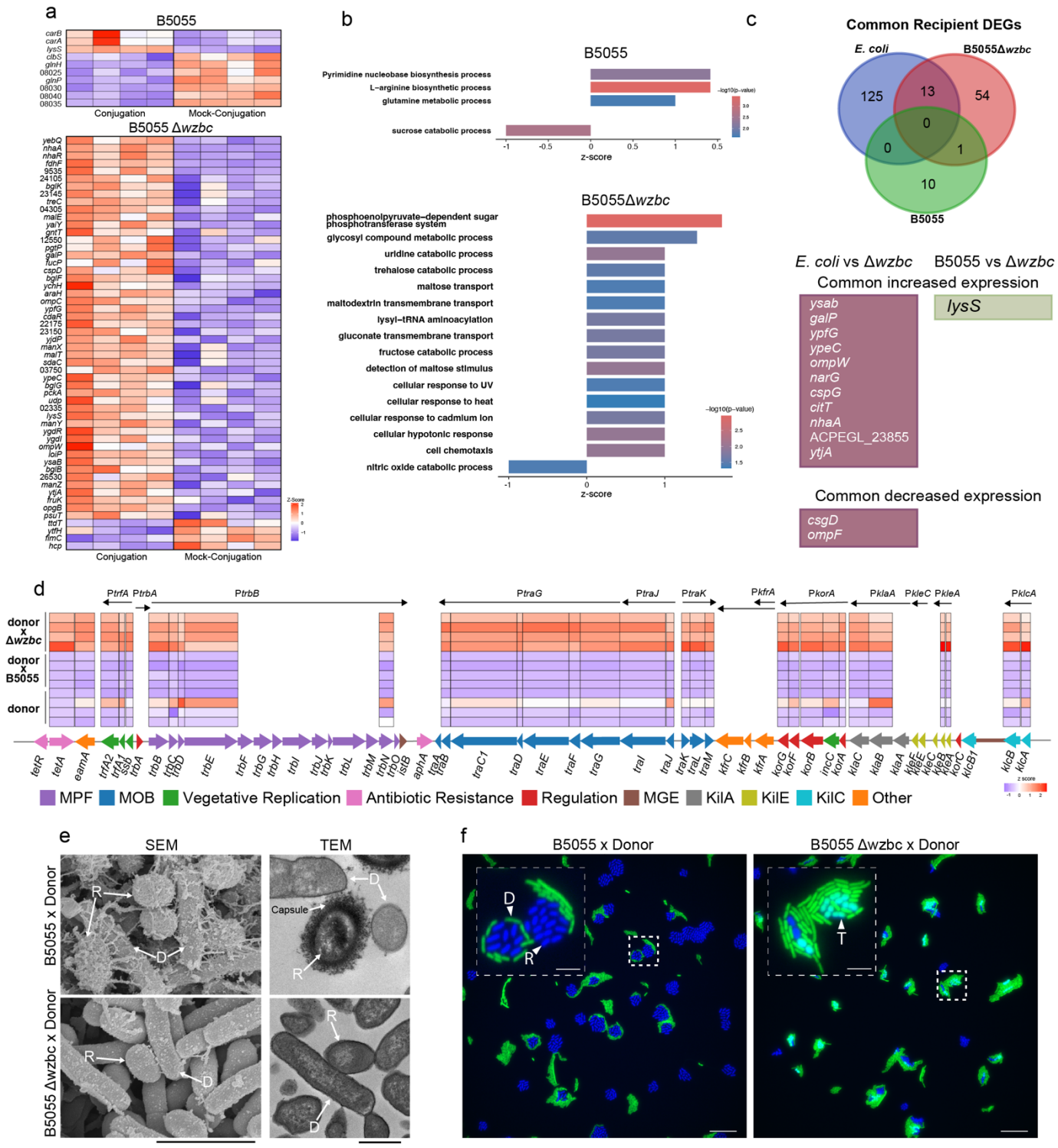
a
B5055
Conjugation
Mock-Conjugation
B5055 Δwzbc
Conjugation
Mock-Conjugation
b
B5055
Pyrimidine nucleobase biosynthesis process
L-arginine biosynthetic process
glutamine metabolic process
sucrose catabolic process
z-score
B5055Δwzbc
phosphoenolpyruvate-dependent sugar phosphotransferase system
glycosyl compound metabolic process
uridine catabolic process
trehalose catabolic process
maltose transport
maltodextrin transmembrane transport
lysyl-tRNA aminoacylation
gluconate transmembrane transport
fructose catabolic process
detection of maltose stimulus
cellular response to UV
cellular response to heat
cellular response to cadmium ion
cellular hypotonic response
cell chemotaxis
nitric oxide catabolic process
z-score
c
Common Recipient DEGs
E. coli
B5055Δwzbc
B5055
125
13
54
0
0
1
10
E. coli vs Δwzbc
B5055 vs Δwzbc
Common increased expression
ysab
galP
ypfG
ypeC
ompW
narG
cspG
citT
nhaA
ACPEGL_23855
ytjA
lysS
Common decreased expression
csgD
ompF
d
donor x Δwzbc
donor x B5055
donor
MPF
MOB
Vegetative Replication
Antibiotic Resistance
Regulation
MGE
KilA
KilE
KilC
Other
e
SEM
TEM
B5055 x Donor
B5055 Δwzbc x Donor
Capsule
R
D
f
B5055 x Donor
B5055 Δwzbc x Donor
D
R
T

751 **Figure 2. The effect and mechanism of capsule on conjugation and the recipient and plasmid**
752 **response. a)** Differentially expressed genes (DEGS) in *K. pneumoniae* B5055 (top) and
753 B5055Δ*wzbc* (bottom) genes during active conjugation or co-culture with an RP4 donor. **b)** GO
754 term analysis of DEG for B5055 (top) and B5055Δ*wzbc*, with raw P-values reported as per TopGO
755 package guidelines for the weight_01 algorithm. **c)** Common DEGS between recipient responses
756 (top), that are increased in expression (middle) or decreased (bottom). **d)** Differentially expressed
757 RP4 genes during active conjugation with B5055Δ*wzbc* (top) B5055 (middle), or the donor alone
758 (bottom). **e)** TEM, and SEM images of conjugation between *K. pneumoniae* B5055 or B5055Δ*wzbc*
759 recipients with *E. coli* LT101. Recipients are distinguished based on the presence of capsule, and
760 shape. **f)** *In situ* visualisation of conjugation between either wildtype or Δ*wzbc* recipients by
761 fluorescent microscopy. All images are representative of ≥2 independent experiments.
762 Abbreviations: D=Donor, R=Recipient, T=Transconjugant. Numbers in *K. pneumoniae* gene lists
763 represent locus tags trimmed of the prefix J6T75_RS. Scale bars: SEM 3 μm, TEM 1 μm,
764 Fluorescence microscopy 20 μm, inset 5 μm.
765

766

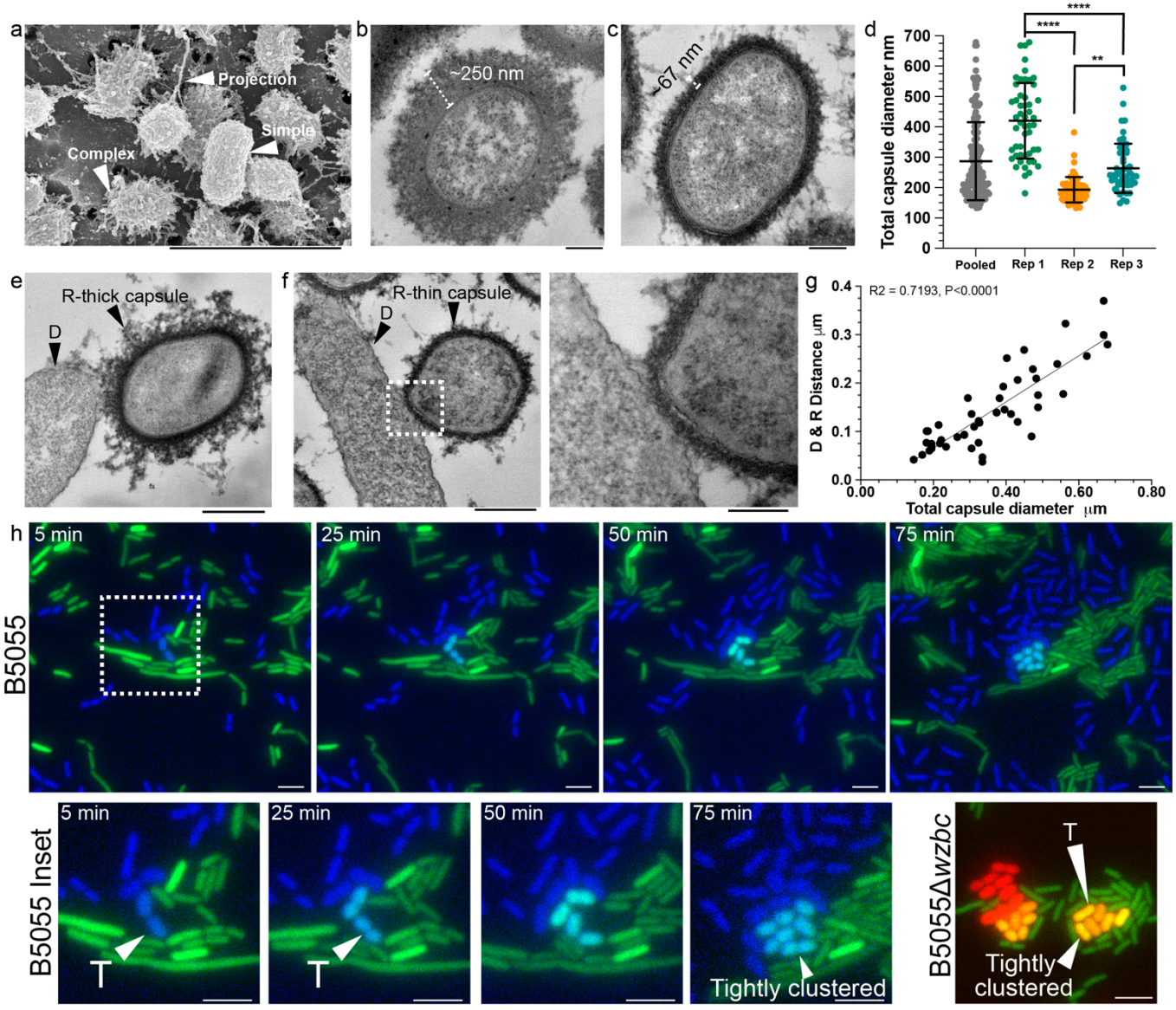
a
Projection
Simple
Complex
b
~250 nm
c
67 nm
d
Total capsule diameter nm
Pooled
Rep 1
Rep 2
Rep 3
****
****
**
e
R-thick capsule
D
f
R-thin capsule
D
g
R2 = 0.7193, P<0.0001
D & R Distance µm
Total capsule diameter µm
h
B5055
5 min
25 min
50 min
75 min
B5055 Inset
T
Tightly clustered
B5055Δwzbc
T
Tightly clustered

767 **Figure 3. Recipient *K. pneumoniae* capsule thickness variation impacts donor-recipient**
768 **interactions and conjugation. a)** SEM imaging of capsular variation and projections. **b-c)** TEM
769 imaging of capsule thickness variation between individual cells. **d)** Variation in capsule thickness
770 within, and between biological replicates (n = ≥50 cells per sample, one-way ANOVA with sidak's
771 multiple comparison testing P-values = ** ≤ 0.01, **** ≤ 0.0001.). **e-f)** Effect of capsule thickness
772 variation on donor-recipient interactions. **g)** Linear regression analysis of distance between outer
773 membrane of donor and recipient and total capsular diameter (R^2=.72, N=47, F-test P≤0.0001). **h)**
774 Live cell imaging of B5055 transconjugant formation, showing that B5055 transconjugants arise
775 from recipients intimately contacting the donor and morphologically resemble acapsular
776 B5055Δ*wzbc*. Error bars = mean ± SD. Scale bars: a = 5 μm, bc = 200 nm, ef = 500 nm, f inset =
777 200 nm, h = 20 μm, h insert = 5 μm. Images are representative of ≥ 2 independent experiments,
778 except for h which depicts the rare formation of a B5055 transconjugant.

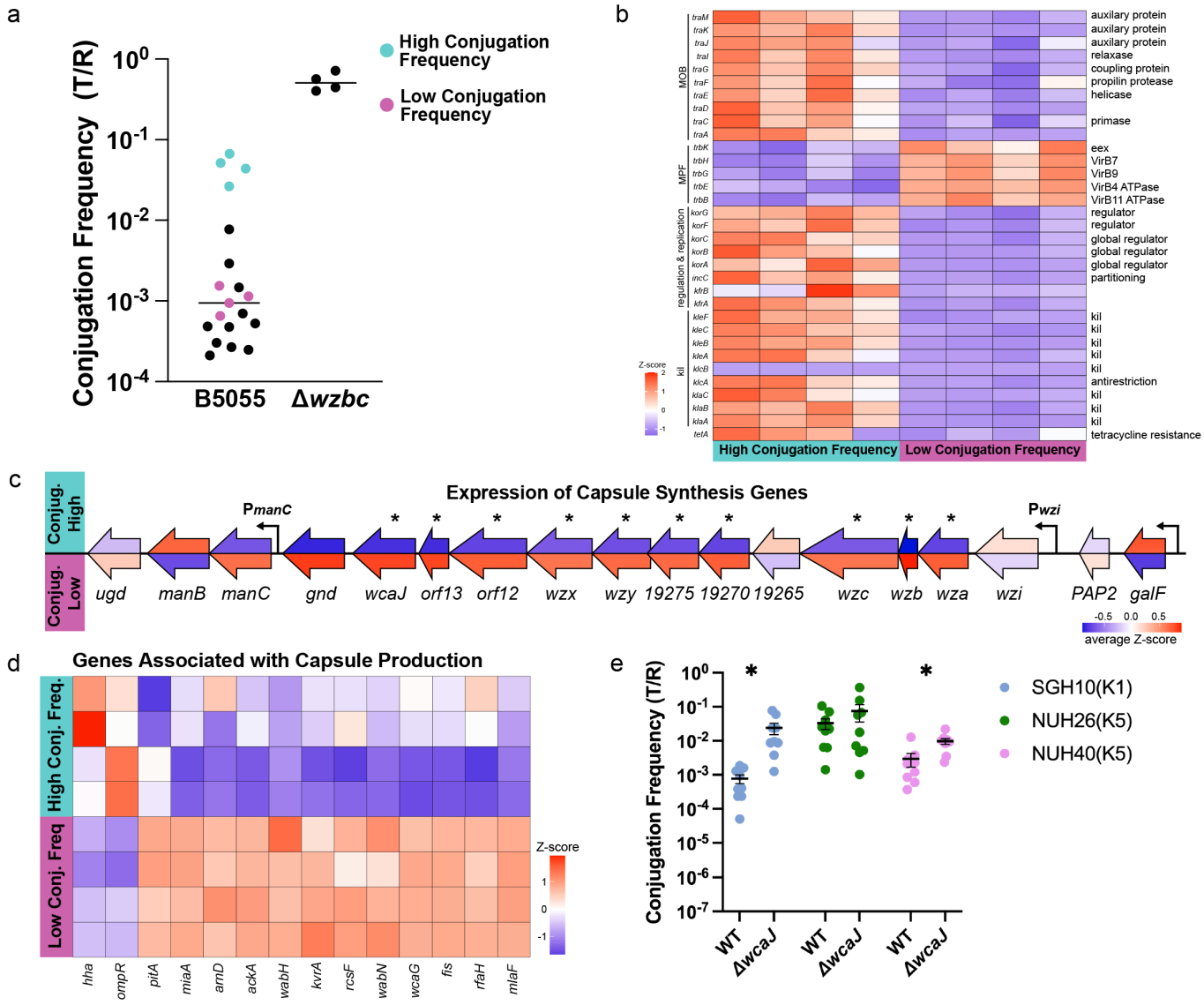
a
Conjugation Frequency (T/R)
High Conjugation Frequency
Low Conjugation Frequency
B5055
Δwzbc
b
MOB
MPF
regulation & replication
kil
traM auxilary protein
traK auxilary protein
traJ auxilary protein
traI relaxase
traG coupling protein
traF propilin protease
traE helicase
traD
traC primase
traA
trbK eex
trbH VirB7
trbG VirB9
trbE VirB4 ATPase
trbB VirB11 ATPase
korG regulator
korF regulator
korC global regulator
korB global regulator
korA global regulator
incC partitioning
kfrB
kfrA
kleF kil
kleC kil
kleB kil
kleA kil
klcB kil
klcA antirestriction
klaC kil
klaB kil
klaA kil
tetA tetracycline resistance
Z-score
High Conjugation Frequency
Low Conjugation Frequency
c
Expression of Capsule Synthesis Genes
Conjug. High
Conjug. Low
PmanC
Pwzi
ugd manB manC gnd wcaJ orf13 orf12 wzx wzy 19275 19270 19265 wzc wzb wza wzi PAP2 galF
average Z-score
d
Genes Associated with Capsule Production
High Conj. Freq.
Low Conj. Freq
hha ompR pitA miaA amD ackA wabH kvrA rcsF wabN wcaG fis rfaH mlaF
Z-score
e
Conjugation Frequency (T/R)
SGH10(K1)
NUH26(K5)
NUH40(K5)
WT
ΔwcaJ

780 **Figure 4. Population level capsule variation enables RP4 conjugation in capsulated *K.***
781 ***pneumoniae*.**
782 **a)** Variation in conjugation frequency of *K. pneumoniae* B5055. The conjugation frequency of
783 B5055Δ*wzbc* is shown for context. **b)** Differential expression of RP4 encoded genes between
784 conjugation high and low samples. **c)** Differential expression of genes in the capsule synthesis
785 locus between conjugation high (top) and low (bottom) samples. **d)** Genes associated with
786 capsule production between samples with high or low conjugation frequencies. **e)** The
787 conjugation frequency of RP4 to hypermucoid K1 or K5 *K. pneumoniae* (N=9, P>.05 Mann-
788 Whitney U test). Data are presented as the median (**a**), or the mean+SEM (**d**).

789

790

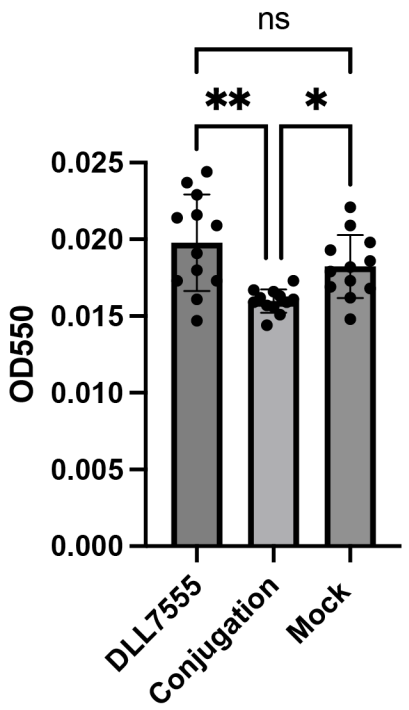

791

792 **Supplementary Figure 1: Donor LT101(pVS520) and Recipient DLL7555 co-culture causes a**
793 **minor reduction in biofilm formation.**

794 Biofilms were grown as in (62). Briefly, 1:100 dilutions of overnight broth cultures of donor, recipient
795 and mock donor in fresh LB medium were mixed in 1:1 in a flat bottomed 96 well tray and grown
796 for 24 hours at 37°C. Outer wells were not used to avoid evaporation effects. Following incubation,
797 the liquid portion of the culture was removed and plated to confirm transconjugants were present
798 and therefore conjugation had occurred. The biofilms were washed in water, and quantitated by
799 staining with 0.1% crystal violet, which after washing was solubilized with 30% acetic acid and
800 measured by absorbance reading at 550 nm standardized against 30% acetic acid. Error bars =
801 mean ± SD, N = 4 biological replicates repeated 3 times). Significance testing was performed with
802 a Kruskal Wallis one way ANOVA with Dunn's multiple comparison testing P-values = *** ≤ 0.01,
803 **** ≤ 0.0001.).

804

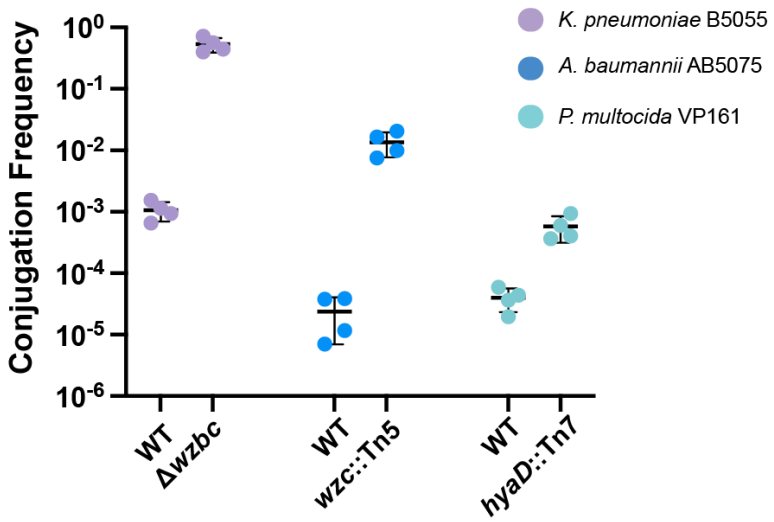

Supplementary Figure 2: Capsule is a barrier to conjugation in diverse species. The conjugation frequency of RP4 or RP4-mobilizable plasmids from *E. coli* LT101 to K. *pneumoniae* B5055, *A. baumannii* AB5075, or *P. multocida* VP161 and their unencapsulated derivatives (Mean±SD, N=4, P>.05 Mann-Whitney U test).

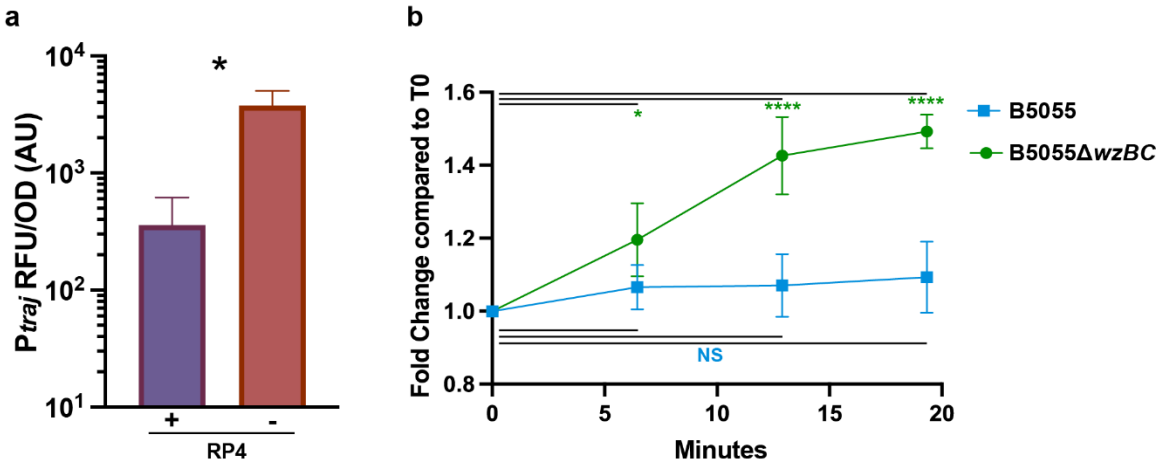

Supplementary Figure 3: Capsule inhibits activation of the RP4 relaxase promoter P*traJ* within the donor. A fluorescent reporter was constructed for the RP4 relaxase promoter P*traJ* by fusing it to three tandem low sequence-homology GFP reporters. Three tandem GFPs were used because fluorescence from 1 GFP reporter could not be detected, likely because P*traJ* is a weak promoter **a)** The presence of RP4 is known to repress P*traJ* and therefore measurement of GFP intensity in the presence or absence of RP4 confirmed the reporter functioned as expected (N = 4, P<0.05, Mann-Whitney U-Test). **b)** Measurement of P*traJ*x3GFP in the donor cell was achieved by performing conjugations in a 96-well tray on agar containing rifampicin which inhibits transcription only in the recipient cell. Significance testing was performed with a one-way ANOVA with Sidak's multiple comparison. Error bars = mean ± SD

823

a

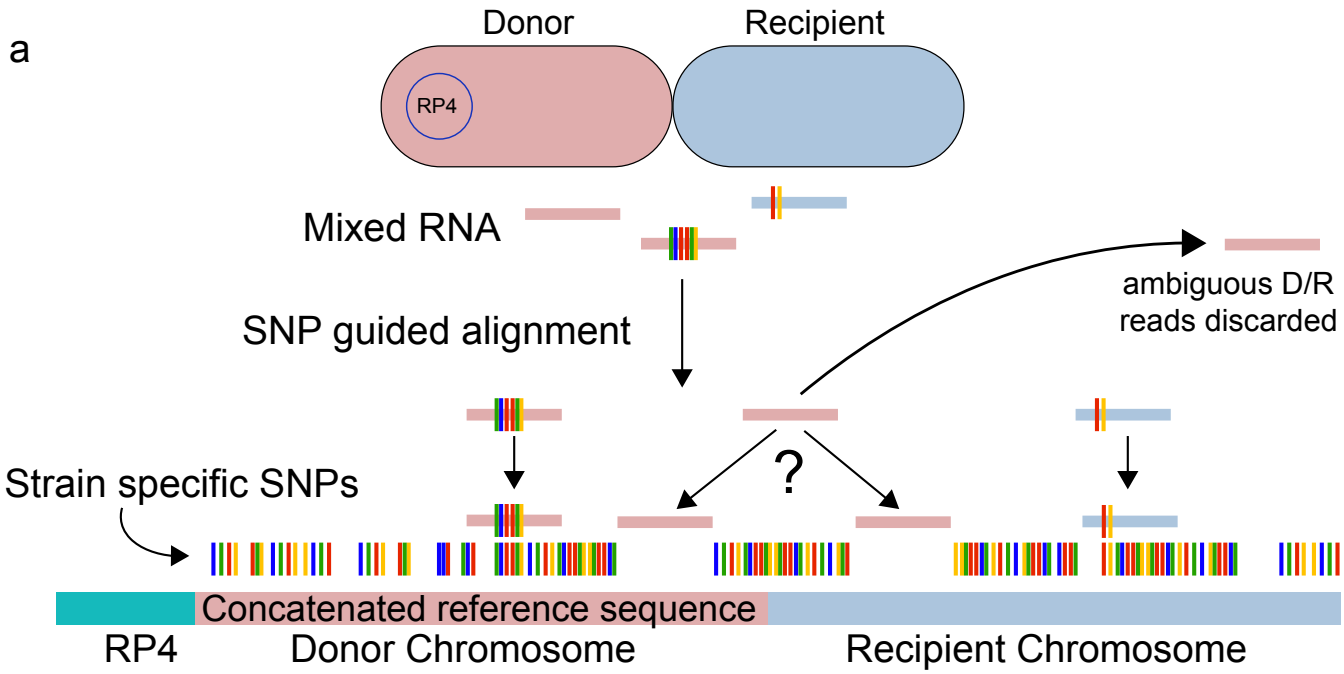
Donor
Recipient
RP4
Mixed RNA
SNP guided alignment
ambiguous D/R
reads discarded
?
Strain specific SNPs
Concatenated reference sequence
RP4
Donor Chromosome
Recipient Chromosome

b

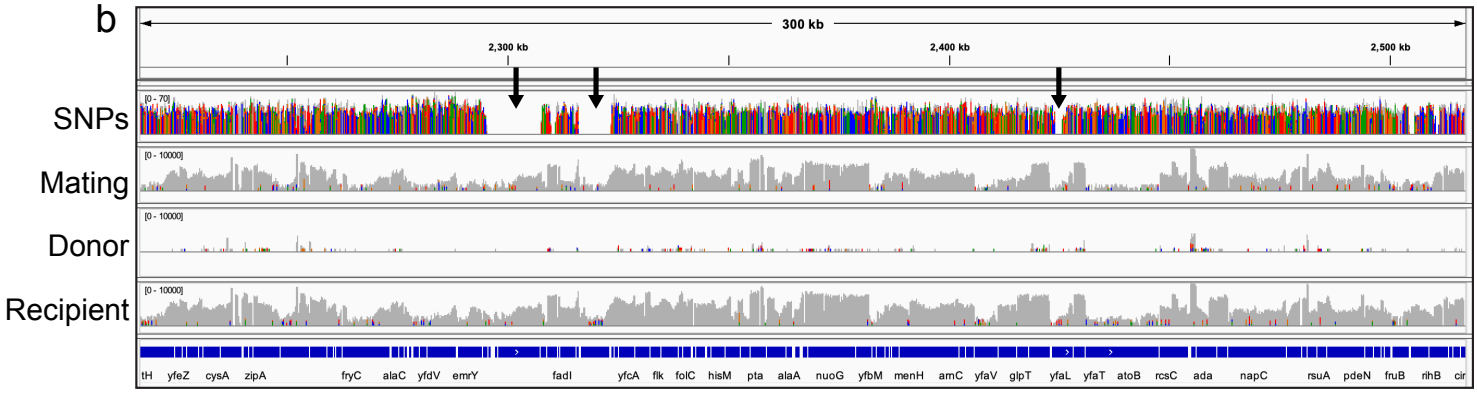
300 kb
2,300 kb
2,400 kb
2,500 kb
SNPs
Mating
Donor
Recipient
tH yfeZ cysA zipA fryC alaC yfdV emrY fadI yfcA flk folC hisM pta alaA nuoG yfbM menH amC yfaV glpT yfaL yfaT atoB rcsC ada napC rsuA pdeN fruB rihB cir

c

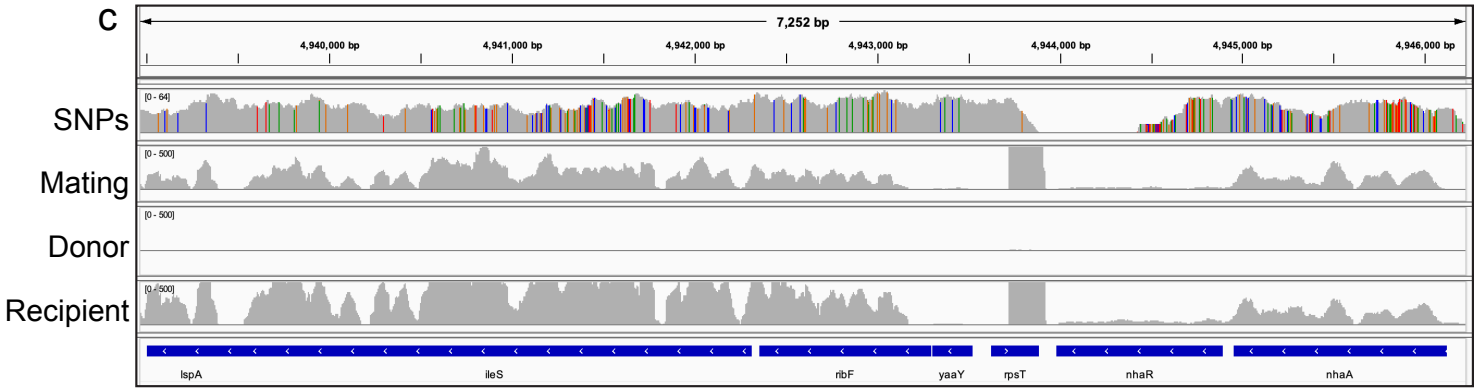
7,252 bp
4,940,000 bp
4,941,000 bp
4,942,000 bp
4,943,000 bp
4,944,000 bp
4,945,000 bp
4,946,000 bp
SNPs
Mating
Donor
Recipient
lspA ileS ribF yaaY rpsT nhaR nhaA

824

825 **Supplementary Figure 4: SNP and RNA-seq read alignment for HB101(pVS520) x DLL7555.**
826 a) Schematic overview of RNA-seq alignment strategy. b-c) IGV plots depicting the coverage of
827 SNPs, and the alignment of mating, pure recipient and pure donor read coverage against a recipient
828 portion of the concatenated reference sequence at a global (b) and local (c) level. Gaps indicated
829 by black arrows in represent genome segments unique to DLL7555. The reads are log scaled in
830 (b).

831

832 **Table 1.** Bacterial strains and plasmids used in this work.

Strain	Genotype/Characteristics	Reference
E. coli		
DH5α	F- φ80*lac*ZΔM15Δ(*lac*ZYA-*arg*F)U169 *rec*A1 *end*A1 *hsd*R17(r_K ,m_K^+) *pho*A *sup*E44λ⁻*thi*-1 *gyr*A96 *rel*A1	Invitrogen
LT101	Rif^R derivative of HB101	(63)
DLL7555	ST73 Rif^R clinical isolate of *E. coli*	(64)
K. pneumoniae		
B5055	Wild type *K. pneumoniae* O1:K2	Provided by Richard Strugnell
B5055Δ*wzbc*	Non-encapsulated *wzbc* deletant mutant of B5055, Km^R	Provided by Richard Strugnell, Adam Jenney, and Tania Uren
SGH10	Hospital isolate of *K. pneumoniae* K1, ST23	(65)
NUH26	Hospital isolate of *K. pneumoniae* K5, ST1049	(66)
NUH40	Hospital isolate of *K. pneumoniae* K5, ST1049	(9)
A. baumannii		
AB5075	Wild type *A. baumanii* KL25, Ap^R, Erm^S	(67)
AB10132	Capsular transposon mutant of AB5075, *wzC*::Tn*5*, Tc^R	(68)
Pasteurella multocida		
AL3145	Km^R derivative of VPI161	(59)
AL2234	VP161 capsular transposon mutant *hyaD*-Tn*7,* Km^R	(59)
Plasmids		
pWSK29	Ap^R, low copy number cloning vector	(69)
pWSK29 P*traJ*GFPx3	P*traJ*::*mGreenLantern*x3	
pSU18	Cm^R, medium copy number cloning vector	(70)
pSU18*mTagBFP2*	P*em7*::*mTagBFP2*	This work
pVS520	Tc^R, Ap^S, Km^S, derivative of RP4; Tra^+ Mob^+	(63)

pMMB67EH	RSF1010 derived expression vector. Ap^R, Mob^+	(71)
RFS1010-*erm*	Erm^R derivative of RSF1010, Mob^+	This work
pAL99S-*oriT*	$Spec^R$, Mob^+ derivative of pAL99S	This work
pMMB67EH*gfpmut3*	P*em7*::*gfpmut3*	This work

833 **Note:** rif = rifampicin, km = kanamycin, tc = tetracycline, ap = ampicillin, cm = chloramphenicol,
834 erm = erythromycin, spec = spectinomycin